Dalton Transactions

RSC Publishing

PAPER

View Article Online
View Journal | View Issue

Amine functionalized K10 montmorillonite: a solid acid–base catalyst for the Knoevenagel condensation reaction

Cite this: *Dalton Trans.*, 2013, **42**, 5122

G. Bishwa Bidita Varadwaj, Surjyakanta Rana and K. M. Parida*

Different amine functionalized K10 montmorillonites were hydrothermally fabricated by a simple method of treatment of the neat clay with different amine solutions and used as heterogeneous catalysts towards the Knoevenagel condensation reaction. Catalytic results show that the di-amine functionalized K10 montmorillonite exhibits high efficacy for promoting this reaction at room temperature and in the absence of a solvent. The solid catalyst was characterized using a variety of different techniques; including Fourier transform infrared spectroscopy (FT-IR), nitrogen physisorption measurements, ^{29}Si CP MAS NMR spectroscopy, NH_3-temperature programmed desorption (NH_3-TPD), X-ray powder diffraction (XRD), and field emission scanning electron microscopy (FESEM). The catalyst could be recycled and reused for several runs without any loss of inherent catalytic activity.

Received 19th October 2012,
Accepted 14th January 2013

DOI: 10.1039/c3dt32495h

www.rsc.org/dalton

1. Introduction

Montmorillonite is a ubiquitous, inexpensive and eco-friendly support, preferred in heterogeneous catalysis.[1,2] Therefore, substantial efforts in research have been made on modified montmorillonites by our group, like pillaring with metal oxides by different techniques, complex immobilization and surface modification with heteropoly acids, *etc*.[3–9] Since surface functionalization on inorganic supports with many organic moieties provides organo-inorganic hybrids, where the inorganic and organic components are linked *via* strong-type interactions (*i.e.* covalent or iono-covalent bonds), we now directed our study to the surface functionalization of clays to fabricate some stable catalysts. This approach enables robust immobilization of the reactive organic groups by strong binding on the clay surfaces, preventing therefore their leaching in the surrounding medium when used in solutions. Consequently, these materials can act as active heterogeneous liquid-phase catalysts without further alteration and also give access to a large variety of potential catalysts by successive chemical derivatization.

Knoevenagel condensation is one of the most useful and widely employed methods for carbon–carbon bond formation with numerous applications in the synthesis of fine chemicals.[10,11] In Knoevenagel condensation, the aldehydes condense with compounds containing active methylene groups, which is usually catalyzed by weak bases like primary, secondary, tertiary amines and ammonium salts under homogeneous conditions.[12,13] Other Lewis acids have also been reported as catalysts in the Knoevenagel condensation, including $ZnCl_2$, Al_2O_3 and KF–Al_2O_3, *etc*.[14–16]

K10 montmorillonite is known to behave as an acid catalyst in organic reactions. Therefore, we thought to employ a new type of solid acid–base catalyst, where the base is covalently grafted onto a solid acidic support towards the desired reaction. Hence, we did mono and di-amine functionalization on K10 montmorillonite and compared their activities towards the Knoevenagel condensation reaction. In our early reports, we carried out the reaction in the absence of a solvent using amine functionalized zirconia and MCM-41.[17,18] However, we are getting better results using the present system for a shorter period of time. This may be due to the interlayer acid sites promoting the base catalyzed reactions in amine functionalized acidified montmorillonite as reported by Motokura *et al*.[19] They varied various solvents and found *n*-heptane as the best solvent for the functionalization. However, taking water as the solvent they observed a high amine loading on acid activated montmorillonite. Therefore, water can be taken as a green alternative solvent for the functionalization of amines on acid activated montmorillonite. Hence in this work, we have chosen a water medium to prepare amine functionalized K10 montmorillonite.

The objective of the present work is to explore the possibility of utilizing K10 montmorillonite as an inexpensive raw material for the preparation of organo-inorganic hybrids by

C&MC Department, Institute of Minerals & Materials, Technology, Bhubaneswar-751013, Orissa, India. E-mail: paridakulamani@yahoo.com; Fax: +91 674 2581637; Tel: +91 674 2581636 (Extn.9425)

grafting them with amino propyl triethoxysilane (APTES) and *N*-(2-amino ethyl)-3-amino propyl trimethoxysilane (AAPTMS), and to evaluate the resulting materials towards the Knoevenagel condensation reaction. The di-amine functionalized catalyst is found to be robust enough to achieve high catalytic activity toward the Knoevenagel condensation reaction at room temperature and also under solvent free conditions in 12 h; *i.e.* beneficial for industry as well as environment, particularly from the viewpoint of green chemistry.

2. Experimental

2.1 Preparation of the catalyst

1 g K10 montmorillonite was added to 15 ml of a solution of 3-amino propyl triethoxysilane (2.32 mmol) using water as a solvent and stirred at room temperature for 2 h. The suspended solution was transferred into a teflon bottle and hydrothermally aged at 100 °C for another 10 h. The solid products were filtered; three times washed with deionized water and dried subsequently in a vacuum at 80 °C for 8 h. It is named as APTES@K10. AAPTMS@K10 is also prepared using the same procedure, taking *N*-(2-amino ethyl)-3-amino propyl trimethoxysilane as the amine source as shown in Scheme 1.

2.2 Characterization techniques

The BET surface area, average pore diameter, mesopore distribution, total pore volume of all the samples were determined by a multipoint N_2 adsorption–desorption method at liquid N_2 temperature (−196 °C) using an ASAP 2020 (Micromeritics) surface area analyser. Prior to analyses, all the samples were degassed at 300 °C and 10^{-6} Torr pressure for 5 h to evacuate the physically adsorbed moisture. The acid character of the samples was studied by an NH_3-TPD Auto Chem-II chemisorption analyzer (Micromeritics) equipped with a thermal conductivity detector (TCD). About 1 g of the powdered sample contained in a quartz "U" tube was degassed at 250 °C for 1 h with ultra-pure nitrogen gas. After cooling the sample to room temperature, NH_3 (20% NH_3 balanced with helium) gas was passed over the sample while it was heated at a rate of 10 °C min^{-1} and the profile was recorded. The low and broad angle XRD patterns of powdered samples were taken in the 2θ range of 5–80° at a rate of 2° min^{-1} in steps of 0.01° (Rigaku Miniflex set at 30 kV and 15 mA) using Cu Kα radiation. The FTIR spectra of the samples were recorded using a Varian 800-FTIR spectrophotometer in a KBr matrix in the range of 4000–400 cm^{-1}. The FE-SEM was performed with a ZEISS 55 microscope. ^{29}Si CP MAS spectra were recorded at 79.49 MHz applying 90° pulses, 300 s pulse delays and 5.0 ms contact time. Both the spectra were obtained by using a Bruker Avance 400 MHz spectrometer.

2.3 Catalytic reaction

The Knoevenagel condensation between benzaldehyde and diethyl malonate using the amine functionalized K10 montmorillonite samples was carried out in a magnetically stirred round-bottom flask. About 10 mmol of benzaldehyde (1.01 ml), 10 mmol of diethyl malonate (1.51 ml) and 0.05 g of catalyst were taken in the reactor and were stirred at room temperature. After 12 h of the reaction, 50 ml of methanol was added in order to solubilize all the organic compounds and again stirred for 10 min. The catalyst was recovered by centrifugation for reuse and the reaction mixture was analyzed off-line on a Shimadzu gas chromatograph (GC-2010).

3. Results and discussion

3.1 Characterization

3.1.1 Elemental analysis. The results of nitrogen elemental analysis of the prepared materials suggest that it was loaded onto the clay at 0.92 mmol g^{-1} and 1.84 mmol g^{-1} for APTES and AAPTMS respectively. These amines may be present as non-linked amines or covalently grafted amines on the surface of montmorillonite. The covalent grafting of amines can be confirmed from various studies given below.

3.1.2 FTIR. The FTIR spectra of K10 montmorillonite, APTES@K10 and AAPTMS@K10 are presented in Fig. 1. The

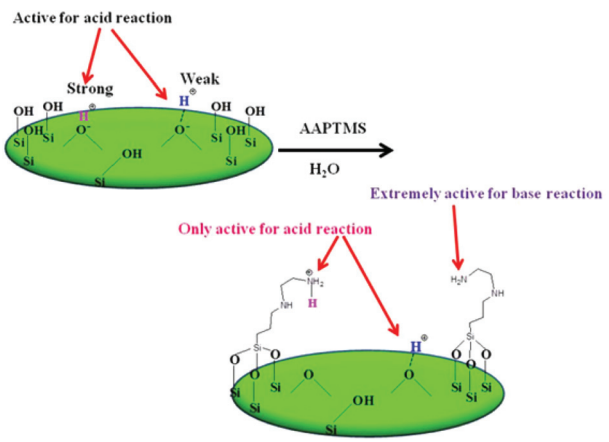

Scheme 1 Mechanism of di-amine immobilization on the K10 montmorillonite surface.

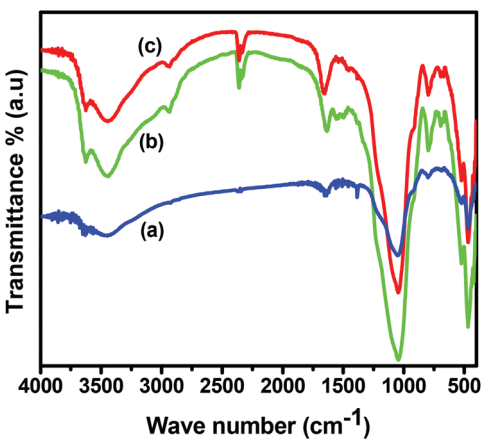

Fig. 1 FTIR spectra of K10 montmorillonite (a), APTES@K10 (b), and AAPTMS@K10 (c).

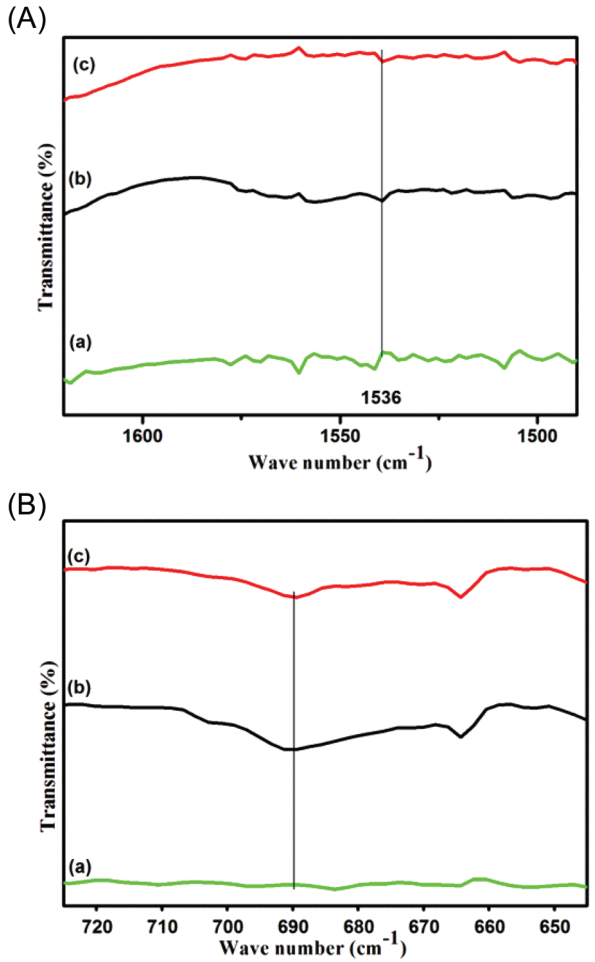

Fig. 2 (A) Enlarged view of the FTIR spectra of K10 montmorillonite (a), APTES@K10 (b), and AAPTMS@K10 (c) showing NH_2 vibrations at 1536 cm^{-1}. (B) Enlarged view of the FTIR spectra of K10 montmorillonite (a), APTES@K10 (b), and AAPTMS@K10 (c) showing NH_2 vibrations at 690 cm^{-1}.

FTIR spectrum of the entire sample shows bands at 3416 and 1636 cm^{-1} for –OH stretching and bending vibrations respectively. The $-CH_2$ stretching and $-CH_2$ bending vibrations from grafted APTES and AAPTMS can be seen in the range 2970–2845 and 1470–1415 cm^{-1} respectively.[20] The presence of N–H bending vibration at around 690 cm^{-1} and of NH_2 symmetric bending vibration at 1536 cm^{-1} (Fig. 2A and 2B) suggests the presence of the organosilanes on the clay surface.

3.1.3 ^{29}Si CP MAS NMR spectroscopy. The ^{29}Si CP MAS NMR spectrum (Fig. 3) provides important information about the degree of functionalization and the coordination environments of the amine moiety with the clay surface. From the solid state NMR spectra, three resonance peaks up-field corresponding to Q^4 (δ = −112 ppm), Q^3 (δ = −101 ppm), and Q^2 (δ = −94 ppm), and two peaks down-field corresponding to T^3 (δ = −68 ppm) and T^2 (δ = −61 ppm), where Q^n = $Si(OSi)_n - (OH)_{4-n}$, n = 2–4 and T^m = $RSi(OSi)_m - (OH)_{3-m}$, m = 1–3 can be observed. The Q^2, Q^3 and Q^4 peaks are the characteristic peaks of the silicate layers present in the clay. The grafting of silane molecules onto the silicate layer of the clay is also

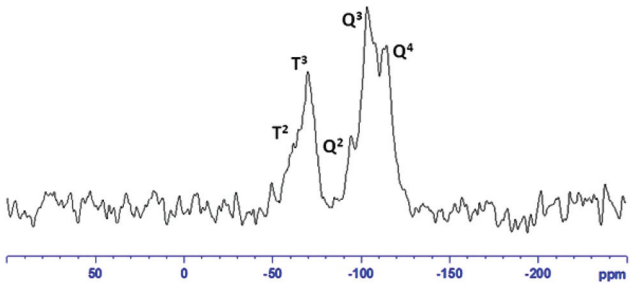

Fig. 3 ^{29}Si CP MAS NMR spectrum of AAPTMS@K10.

supported by the appearance of silicon peaks associated with the silanes in the so-called T region. The presence of T^3 and T^2 peaks confirmed the existence of the covalent linkage between the organic silane moieties of the amine group and the silicate layers of the clay. The high intensity of the T^3 peak reveals the high degree of condensation of the diamine moiety with the clay surface. This confirms the successful covalent attachment of AAPTMS on the surface of the clay.

3.1.4 Nitrogen physisorption studies. N_2 adsorption–desorption is a common method to characterize porous materials, which can provide information about the specific surface area, average pore diameter and pore volume, *etc.* N_2 adsorption–desorption isotherms of K10 montmorillonite, APTES@K10 and AAPTMS@K10 samples are shown in Fig. 4. According to the BDDT classification, all the samples are of type IV with a typical hysteresis loop, featuring mesoporous materials with highly uniform pore size distribution.[21]

BET surface area, pore size and pore volume for different materials are presented in Table 1. The BET surface areas for the APTES@K10 and AAPTMS@K10 samples are 153.15 $m^2\ g^{-1}$ and 140.89 $m^2\ g^{-1}$ respectively, with corresponding pore volumes 0.30 and 0.29 $cm^3\ g^{-1}$ respectively. While a decrease in the surface area and pore volume was observed, we also observed an increase in pore diameter in the case of APTES@K10 (7.9 nm) and AAPTMS@K10 (8.6 nm) than the

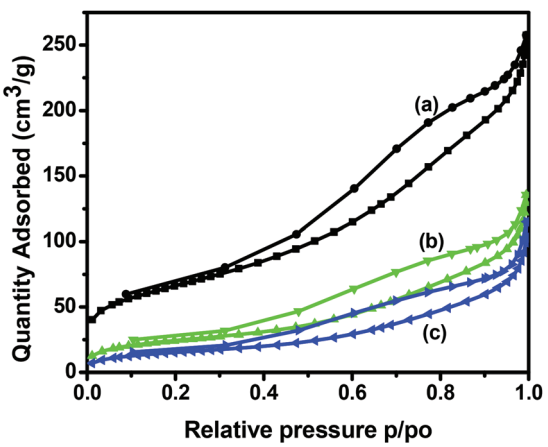

Fig. 4 N_2 ads–des isotherms of K10 montmorillonite (a), APTES@K10 (b), and AAPTMS@K10 (c).

Table 1 Textural data of various samples

Catalyst	Surface area ($m^2\ g^{-1}$)	Pore volume ($cm^3\ g^{-1}$)	Pore diameter (nm)	Total acidity ($mmol\ g^{-1}$)
K10 montmorillonite	242.21	0.41	6.5	4.3
APTES@K10	153.15	0.30	7.9	2.9
AAPTMS@K10	140.89	0.29	8.6	2.5

parent K10 montmorillonite (6.7 nm). A considerable decrease in the BET surface area, and pore volume than the parent K10 montmorillonite suggests the possibility that the organic moieties might have been anchored on the inner surface of the mesopores.

3.1.5 NH_3-TPD. Ammonia TPD is a commonly used method to determine the total acidity of solids, though this method lacks selectivity because ammonia can titrate acid sites of any strength and type. The amount of ammonia desorbed at some characteristic temperatures is taken as a measure of the number of acid centres while the temperature range in which ammonia is desorbed is an indicator of the strength of such acid sites. However, the total acidity values, determined by the temperature programmed desorption of ammonia, are lower for APTES@K10 and AAPTMS@K10, than that of neat K10 montmorillonite (Table 1). The decrease in acidity may be interpreted as: grafting of the organosilane lowers the number of free surface Si–OH groups as well as the strong acidic H^+ ions present in the interlayer space, which are responsible for the acidity in the neat K10 montmorillonite.

3.1.6 XRD. XRD analysis was carried out directly on the raw K10 montmorillonite as well as on the organofunctional clays (Fig. 5 and 6). The corresponding patterns are indicative of a chief contribution of the mineral family corresponding to a typical smectite "montmorillonite". The *hkl* and two dimensional *hk* reflections for montmorillonite can be clearly visualized in all the samples. Apart from these peaks, several peaks due to many impurities like quartz, cristobalite and feldspar can be seen in the diffractograms. A similar nature in the spectrum of the three samples suggests no structural change in the clay matrix.

The suggestive indication of the presence of the organosilanes in the interlayer space cannot be envisaged from the low angle XRD patterns because of the absence of the (001) peak in the neat K10 montmorillonite itself. The poor long range ordering may be due to the damage to the clay layers caused during acid treatment of the synthetic clay. The peak observed at 9° creating doubt about the (001) peak is due to the illite impurity present in the clay.

3.1.7 FESEM. Field emission scanning electron micrographs of K10 montmorillonite, APTES@K10 and AAPTMS@K10 are shown in Fig. 7. FESEM observation reveals that the parent K10 montmorillonite is a layered material consisting of many parallel arrays of cleaved plates. The morphologies of the final products were quite similar to that of the parent clay, as can be seen from the inset of Fig. 7(a). The

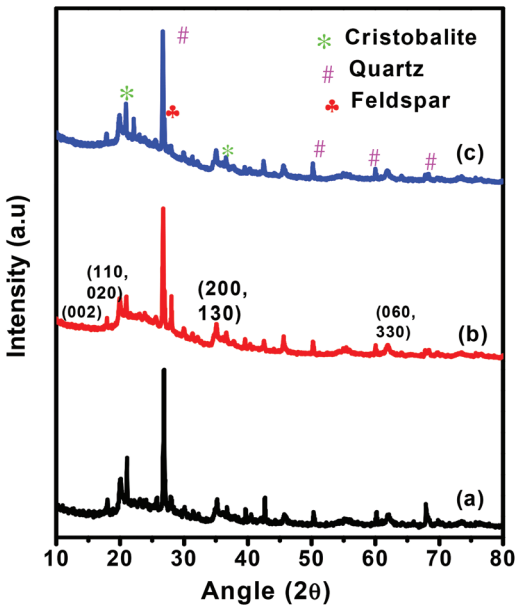

Fig. 5 Broad angle XRD spectra of K10 montmorillonite (a), APTES@K10 (b), and AAPTMS@K10 (c).

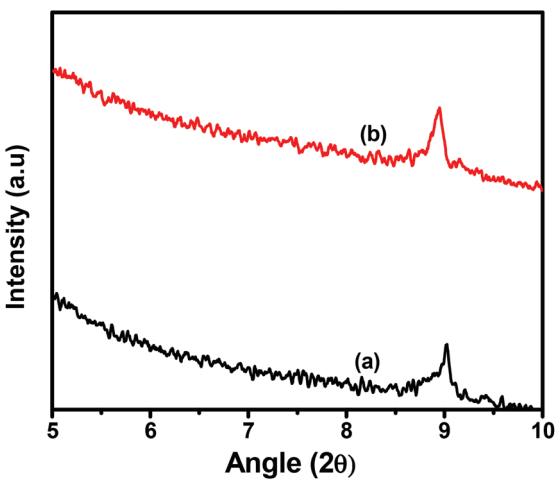

Fig. 6 Low angle XRD spectra of K10 montmorillonite (a) and AAPTMS@K10 (b).

micrographs of APTES@K10 and AAPTMS@K10 clearly show highly porous morphology.

3.2. Catalytic activity

The catalytic activity of the amine modified K10 montmorillonite was assessed for the Knoevenagel condensations of benzaldehyde with diethyl malonate to produce cinnamic acid as the major product. Earlier, Romero *et al.*[22] reported amine-functionalized SBA-15 giving 98% conversion at 105 °C towards the Knoevenagel condensation reaction. However, at room temperature amine-functionalized MCM-41 showed 81% conversion as reported by Sugi *et al.*[23] In our earlier studies with amine functionalised zirconia, we observed

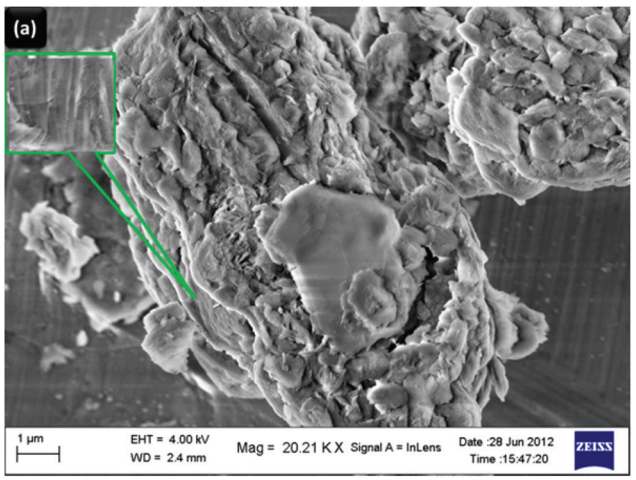

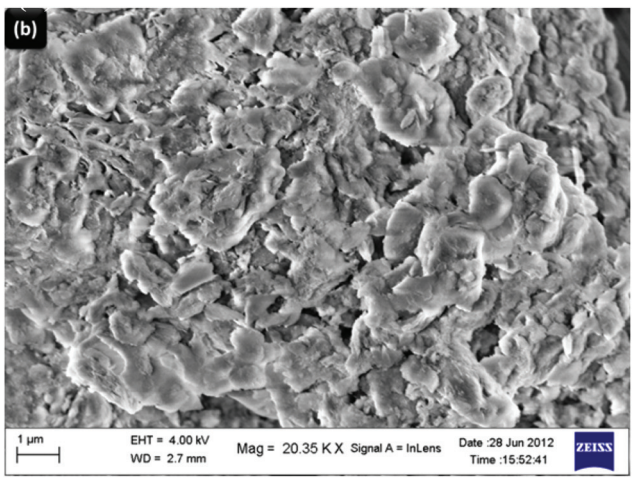

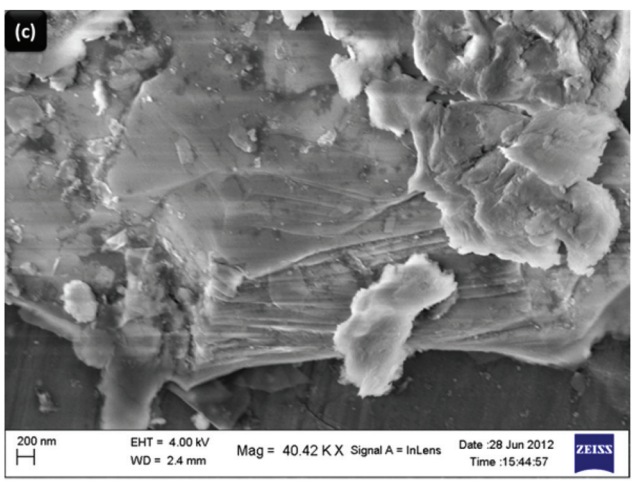

Fig. 7 FESEM images of AAPTMS@K10 (a), APTES@K10 (b), and K10 montmorillonite (c).

89% conversion with 98% selectivity for cinnamic acid and in the case of amine functionalized MCM-41, we got 92% conversion and 98% selectivity in 24 h.[16,17] The inherent disadvantages associated with these reports were either higher temperature or longer reaction time. However, in this study we got better results due to the co-operative effect of the acidic and basic sites present in the amine grafted montmorillonite.

Table 2 Conversion and selectivity of various catalysts towards the Knoevenagel condensation reaction

		Selectivity (%)	
Catalyst	Conversion (%)	Cinnamic acid	Other
K10 montmorillonite	39	97	3
APTES@K10	93	98	2
AAPTMS@K10	97	99	1

As motivated by the principles of green chemistry, it was decided to carry out the reaction under room temperature and solvent free conditions. Initially it was found that no reaction occurred in the absence of any catalyst, whereas K10 montmorillonite grafted with amines or di-amines effectively catalyzed Knoevenagel condensation reactions producing cinnamic acid in high yields, whereas a lower conversion but good selectivity was achieved by unpromoted pure K10 montmorillonite (Table 2). This may be due to the presence of some Lewis acidic sites in neat K10 montmorillonite, which is responsible for the activity. In comparison to the monoamine functionalized K10 montmorillonite, the diamine functionalized catalyst showed highest conversion (97%) due to the presence of more basic sites or increase in nitrogen content. Recently, Park *et al.* demonstrated the use of high nitrogen containing mesoporous carbon nitride as a base catalyst for Knoevenagel condensation of ethylcyanoacetate with aromatic aldehydes.[24]

With such results in hand, we then decided to investigate the effects of various reaction parameters on the condensation of benzaldehyde with diethyl malonate to produce cinnamic acid using AAPTMS@K10 as a catalyst.

The effect of a benzaldehyde to diethyl malonate molar ratio on the reaction conversion was studied by carrying out the reaction at molar ratios of 1 : 4, 1 : 3, 1 : 2, and 1 : 1 respectively (Fig. 8). At a benzaldehyde : diethyl malonate molar ratio of 1 : 2, the catalyst gave the best conversion of 97% in 12 h. The selectivity towards cinnamic acid was 99%. However, on further increasing the diethyl malonate concentration, though the conversion remains almost the same, the product selectivity towards cinnamic acid decreased. This suggests that the self-condensation of diethyl malonate takes place when its concentration in the reactant mixture increases.

In our next move, we then decided to study the influence of the catalyst amount from 0.02 to 1.00 g (Fig. 9). As expected, increasing the amount of AAPTMS@K10 from 0.02 to 0.05 g could lead to a significant enhancement of the conversion (from 76%–97%). It can be clearly seen that the selectivity was meanwhile largely influenced by the catalyst amount, and increasing the catalyst concentration would give higher selectivity. The phenomenon could be attributed to the suppression of the by-product of cinnamic acid with the increase in basicity of the reaction system.

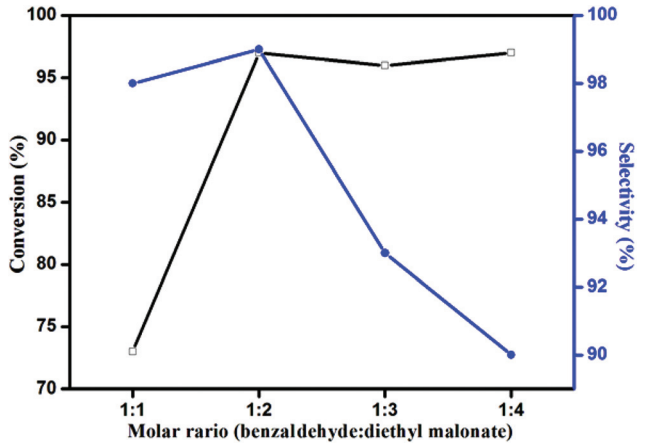

Fig. 8 The effect of molar ratios of benzaldehyde : diethyl malonate towards Knoevenagel condensation. Reaction conditions: room temperature; catalyst amount 0.05 g; time 12 h.

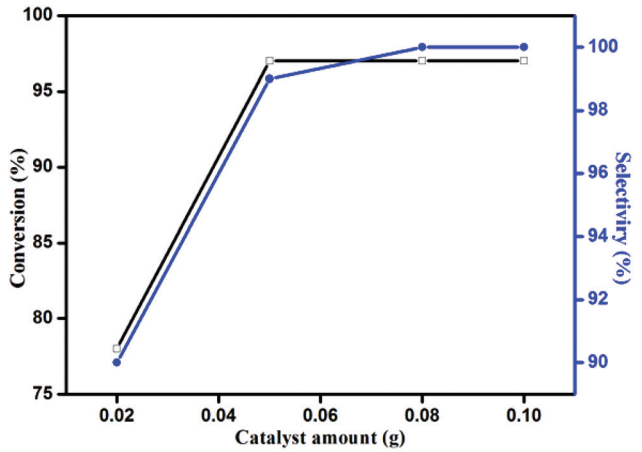

Fig. 9 The effect of catalyst amount towards Knoevenagel condensation. Reaction conditions: room temperature; benzaldehyde : diethyl malonate 1 : 2; time 12 h.

Results showing the influence of reaction time on conversion and product selectivity in the condensation reaction over the AAPTMS@K10 catalyst are presented in Fig. 10. As can be seen from the figure, the conversion and selectivity are increasing with time up to 12 h. Then the reaction became slower and reached a plateau. The conversion and selectivity values show no appreciable change with further rise in reaction time.

The AAPTMS@K10 catalyst was employed in the reaction, where the catalyst activity is mainly due to the structural basicity of the amine group. The reaction pathway can be rationalized by the possible mechanism illustrated in Scheme 2. The scheme shows a co-operative effectiveness of a single clay based system containing acid and basic sites in it.[25] The acid sites present in the clay activate the carbonyl (benzaldehyde), and the basic sites activate the diethyl malonate, this on subsequent steps of the Knoevenagel condensation produces cinnamic acid and condensation products of diethyl malonate.

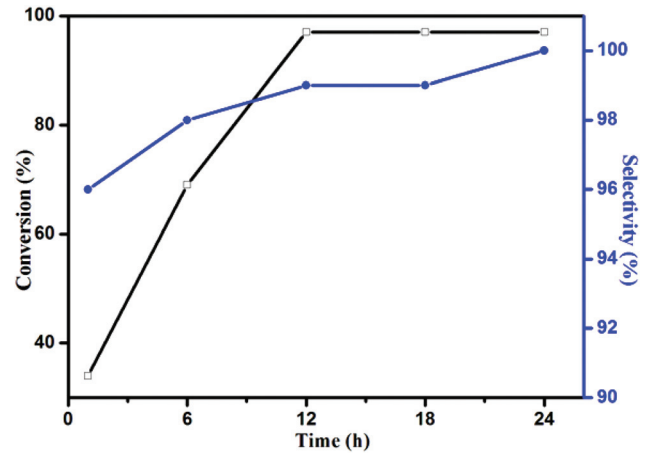

Fig. 10 Influence of reaction time on Knoevenagel condensation. Catalyst amount, 0.05 g; room temperature; benzaldehyde : diethyl malonate 1 : 2.

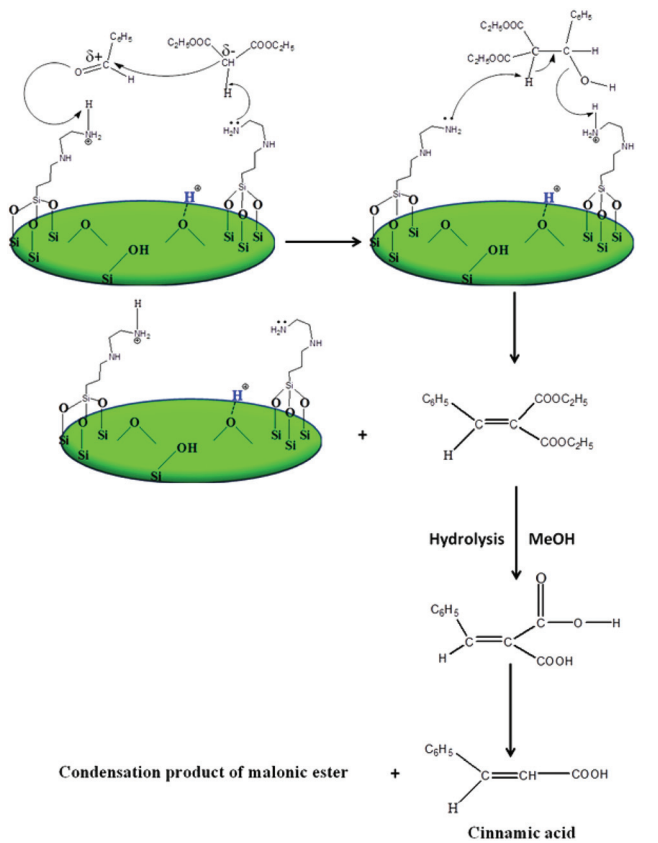

Scheme 2 A plausible reaction mechanism for the Knoevenagel condensation by AAPTMS@K10.

In order to demonstrate the versatility of AAPTMS@K10 for Knoevenagel condensation, we submitted various substituted aldehydes and substrates containing active methylene groups with the molar ratio 1 : 2.

In the case of substituted benzaldehyde containing electron donating groups (–CH_3, *etc.*), the conversion decreased while the electron withdrawing substituents (NO_2, –CN, *etc.*) on the

Table 3 Knoevenagel condensation of various aldehydes with diethyl malonate under solvent free conditions

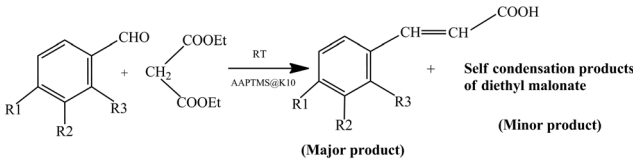

Sl. no	R1	R2	R3	Conversion (%)	Selectivity (%) Major	Minor
1	OH	—	—	85	91	9
2	—	—	CH_3	81	87	13
3	—	NO_2	—	98	99	1
4	—	—	CN	99	99	1
5	H	H	H	97	99	1

Conditions: room temperature, catalyst – 0.05 g, time – 12 h, substituted benzaldehyde: substrates possessing active methylene groups 1 : 2.

Table 4 Effect of various active methylene groups towards Knoevenagel condensation

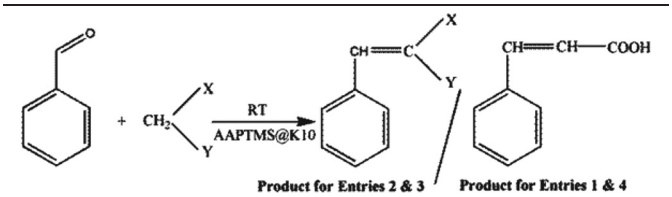

Sl. no	X	Y	Conversion (%)	Selectivity (%) Major	Minor
1	COOEt	COOEt	97	99	1
2	CN	CN	99	99	1
3	CN	COOEt	93	95	5
4	COOMe	COOMe	82	87	13

Conditions: room temperature, catalyst – 0.05 g, time – 12 h, benzaldehyde: compounds containing active methylene groups 1 : 2.

aromatic ring substantially increased the conversion (Table 3). In the case of electron withdrawing groups the possibility of attack of the carbanion (generated from the active methylene group) on the carbonyl carbon is more when compared to that of electron donating groups.

Condensation of benzaldehyde with various substrates possessing active methylene groups is shown in Table 4. The substituents with electron withdrawing nature stabilize the carbanion (due to resonance) compared to those having electron donating nature. So malononitrile displays the maximum conversion among all other substrates.

3.2.1 Recycling test. To reduce the cost of production in chemical industries, now-a-days researchers are keener towards the development of effective heterogenized catalytic systems, which can be reused for several cycles. In this context,

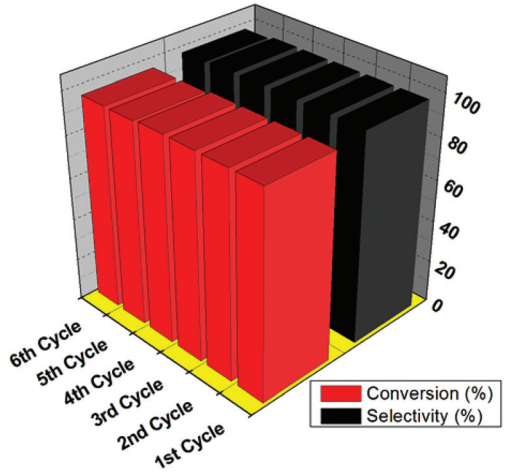

Fig. 11 Results of recycling tests.

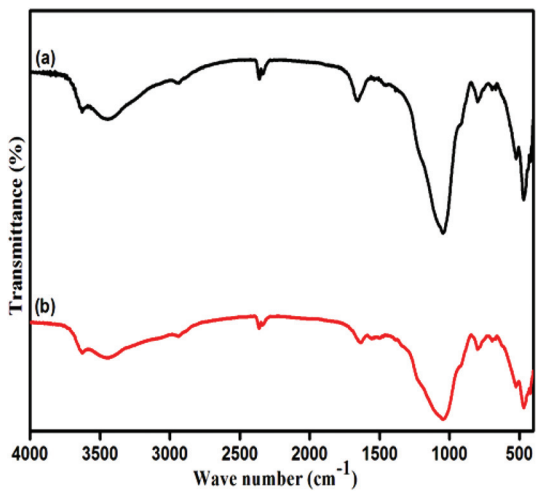

Fig. 12 FT-IR spectra of fresh AAPTMS@K10 (a) and reused AAPTMS@K10 (b).

Fig. 11 shows the recycling test of the AAPTMS@K10 catalyst towards the Knoevenagel condensation. The catalyst was separated by centrifugation after the reaction, washed several times with distilled water, dried, and used in the reaction with a fresh reaction mixture. No significant decrease in either activity or selectivity was observed after being used repetitively for 6 times. This can be attributed to the strong covalent bonding of the amine moiety with the clay surface. Comparison of the FTIR spectra of the fresh and reused catalyst persuasively validates that the structural reliability of the AAPTMS@K10 remains unchanged after the Knoevenagel condensation reaction (Fig. 12).

4. Conclusion

We have synthesized two catalytic systems APTES@K10 and AAPTMS@K10 based on the functionalization of K10 montmorillonite. Furthermore, such systems require minimum

effort for preparation using a simple approach. Under very benign reaction conditions without the help of any solvent, AAPTMS@K10 showed intrinsic high reactivity with 97% conversion and 99% product selectivity in 12 h towards the Knoevenagel condensation reaction. Application of this stable catalyst will be more desirable in industries, since it can be recycled many times without appreciable loss of catalytic activity. A thorough understanding of the behaviour of acidic and basic sites in a single material will open innovative potentials of the material towards one-pot reaction sequences, which is our future prospect.

Acknowledgements

The authors are extremely thankful to Professor B. K. Mishra, Director, CSIR-IMMT, Bhubaneswar 751013, Odisha, India, for his constant encouragement and permission to publish this work. GBBV and SKR are obliged to CSIR for a senior research fellowship.

Notes and references

1 P. Laszlo, *Science*, 1987, **235**, 1473.
2 A. Vaccari, *Catal. Today*, 1998, **41**, 53.
3 T. Mishra and K. M. Parida, *J. Mater. Chem.*, 1997, **7**, 147.
4 T. Mishra and K. M. Parida, *Appl. Catal., A*, 1998, **174**, 91.
5 T. Mishra, P. Mohapatra and K. M. Parida, *Appl. Catal., B*, 2008, **79**, 279.
6 K. M. Parida, G. B. B. Varadwaj, S. Sahu and P. C. Sahoo, *Ind. Eng. Chem. Res.*, 2011, **50**, 7849.
7 G. B. B. Varadwaj, S. Sahu and K. M. Parida, *Ind. Eng. Chem. Res.*, 2011, **50**, 8973.
8 G. B. B. Varadwaj and K. M. Parida, *Catal. Lett.*, 2011, **141**, 1476.
9 G. B. B. Varadwaj, S. Rana and K. M. Parida, *Chem. Eng. J.*, 2013, **215–216**, 849.
10 G. Marciniak, A. Delgado, G. Leclerc, J. Velly, N. Decker and J. Schwartz, *J. Med. Chem.*, 1989, **32**, 1402.
11 D. Enders, E. Muller and A. S. Demir, *Tetrahedron Lett.*, 1988, **29**, 6437.
12 E. Knoevenagel, *Chem. Ber.*, 1894, **27**, 2345.
13 G. Jones, *Org. React.*, 1967, **15**, 204.
14 P. S. Rao and R. V. Venkataratnam, *Tetrahedron Lett.*, 1991, **32**, 5821.
15 F. Texier-Boullet and A. Foucaud, *Tetrahedron Lett.*, 1982, **23**, 4927.
16 G. Dai, D. Shi, L. Zhou and Y. Huaxue, *Chin. J. Appl. Chem.*, 1995, **12**, 104.
17 K. M. Parida, S. Mallick, P. C. Sahoo and S. K. Rana, *Appl. Catal., A*, 2010, **381**, 226.
18 K. M. Parida and D. Rath, *J. Mol. Catal. A: Chem.*, 2009, **310**, 93.
19 K. Motokura, M. Tada and Y. Iwasawa, *J. Am. Chem. Soc.*, 2009, **131**, 7944.
20 E. T. Vandenberg, L. Bertilsson, B. Liedberg, K. Uvdal, R. Erlandsson, H. Elwing and I. Lundstrom, *J. Colloid Interface Sci.*, 1991, **147**, 103.
21 S. Brunauer, L. S. Deming, W. E. Deming and E. Teller, *J. Am. Chem. Soc.*, 1940, **62**, 1723.
22 M. D. Gracia, M. J. Jurado, R. Luque, J. M. Campelo, D. Luna, J. M. Marinas and A. A. Romero, *Microporous Mesoporous Mater.*, 2009, **118**, 87.
23 Y. Kubota, Y. Nishizaki, H. Ikeya, M. Saeki, T. Hida, S. Kawazu, M. Yoshida, H. Fujii and Y. Sugi, *Microporous Mesoporous Mater.*, 2004, **70**, 135.
24 M. B. Ansari, H. Jin, M. Parvin and S.-E. Park, *Catal. Today*, 2012, **185**, 211.
25 M. Zhang, P. Zhao, Y. Leng, G. Chen, J. Wang and J. Huang, *Chem.–Eur. J.*, 2012, **18**, 12773.